Psychoacoustic analysis of the perceptual influence of rotational speed fluctuations in an urban mobility vehicle with distributed ducted fans

Merino Martinez, R.; Schade, Stephen

Publication date
2025

Document Version
Final published version

Published in
Proceedings of the 54th International Congress and Exposition on Noise Control Engineering

Psychoacoustic analysis of the perceptual influence of rotational speed fluctuations in an urban mobility vehicle with distributed ducted fans

Roberto Merino-Martinez[1]
Faculty of Aerospace Engineering, Delft University of Technology
Kluyverweg 1, 2629 HS Delft, The Netherlands

Stephen Schade[2]
Institute of Propulsion Technology, German Aerospace Center.
Bismarckstraße 101, 10625 Berlin, Germany

ABSTRACT

Novel propulsion concepts are being developed for urban air mobility (UAM). This study analyses the noise emissions of a virtual UAM vehicle equipped with 26 distributed, ducted, low-speed fans. Synthetic flyover sounds are generated using an auralization framework, which involves noise predictions, sound propagation, and the binaural audio rendering at the observer position. Since noise emissions of distributed propulsion are characterized by interference effects, this paper discusses the influence of rotational speed fluctuations of the distributed fans on the sound perception of the auralized sounds. These rotational speed fluctuations are modelled as different ranges of random and constant deviations from the nominal speed, in contrast to the baseline case with the 26 fans operating synchronously. The results of a listening experiment performed to evaluate the perceptual differences between the different configurations seem to indicate that relatively small fluctuations in the rotational speed of the fans (e.g. ±1% with respect to the nominal rpm) already notably improve the perceived noise annoyance. The observed differences in annoyance ratings are reasonably well explained by sound metrics that consider the tonal nature of sound, such as the effective perceived noise level (EPNL), tonality, and the psychoacoustic annoyance model by Di et al.

1. INTRODUCTION

Distributed propulsion systems with a typically large number of propulsors are a promising concept in future aircraft designs, including Urban Air Mobility (UAM) vehicles and electric aviation designs, since they provide new degrees of freedom compared to conventional configurations equipped with only a few engines. The number, design, installation, and individual operation conditions [1] of the engines can be modified. For example, for distributed propulsion systems in which each propulsor (e.g. propeller or fan) is powered by an individual motor, the propulsors can be used for both thrust generation and as a flight control system. Consequently, these design variations cause new acoustic

[1]r.merinomartinez@tudelft.nl (corresponding author)

[2]stephen.schade@dlr.de

and psychoacoustic characteristics that will likely affect the noise perception of these devices [2, 3]. This is partly due to potential acoustic interference, modulation, and shielding effects. As a result, the noise emissions from these devices will significantly differ from those of conventional aircraft [4, 5]. Moreover, UAM vehicles are expected to fly at lower altitudes than conventional aircraft, resulting in reduced atmospheric absorption effects and, hence, the high-frequency noise and sharpness are likely crucial for the perception of UAM noise [5]. Overall, noise perception is expected to be a key factor for the societal acceptance of UAM [6, 7]. Hence, in order to design devices that take into account human perception to achieve minimum noise impact [6], it is essential to investigate the noise emissions generated by distributed propulsion systems, as well as their psychoacoustic characteristics, already in the early design stages.

The acoustic design of propulsors is typically based on the sound power level [8, 9]. The noise certification process for new aircraft also employs a single metric, normally the Effective Perceived Noise Level (EPNL) measured at take-off, approach, and flyover [10, 11]. In general, designs with lower cumulative EPNL than a reference value are targeted. However, the design with the lowest EPNL value may not necessarily correspond to the least annoying aural perception [12,13]. Thus, newer aircraft may not necessarily sound more pleasant, even if they have a lower EPNL than conventional aircraft [14]. For these reasons, noise emissions need to be assessed in order to ensure that new propulsion systems are not only quieter than previous concepts but also sound more pleasant, especially when considering distributed propulsion. In fact, human sound perception has been shown to not only depend on purely physical quantities (e.g. sound pressure or sound power level) but to a significant extent also on psychoacoustic characteristics, e.g. sharpness, spectral content and tonality for both conventional turbofan aircraft [15] and multicopter drone platforms [5, 13]. Psychoacoustic sound quality metrics [16,17] are expected to be better predictors of human perception than conventional pressure-based metrics. Ideally, the preferred approach for sound assessment is to conduct listening experiments with human subjects to obtain their subjective responses to different sounds. This is, however, only feasible once the number of designs under consideration is not too large, due to practical reasons [18].

The current paper examines the noise perception of a distributed, ducted fan propulsion system for a UAM vehicle powered by 26 fan engines. In particular, the effect of variations in the rotational speed of individual fans (ΔN) on human perception is investigated. This would be the case for distributed propulsors employed as a flight control system, where rotational speed variations could intentionally be applied to achieve a particular flight condition. In addition, small random rotational speed variations in real applications could also occur if not all motors are perfectly synchronized and due to practical imperfections. Such rotational speed variations or fluctuations can lead to modulation effects with low modulation frequencies, which in turn result in tonal loudness fluctuations and, thus, affect the psychoacoustic characteristics of the propulsion system [19].

To evaluate the UAM vehicle sounds, an analytical auralization (the acoustical counterpart of visualization [20]) framework, developed in-house at the Department of Engine Acoustics of the German Aerospace Center (DLR), is applied to the vectored thrust system of the UAM vehicle under consideration. The fan noise emissions are determined using RANS-informed analytical noise predictions and are then propagated through the atmosphere to specified virtual microphone positions on the ground using virtual flyover simulations. The flyovers are then auralized using binaural noise synthesis. The current study reports the results of a listening experiment campaign that aims to validate the preliminary findings by Schade *et al.* [21], who studied the impact of the rotational speed fluctuations in the individual ducted fans of the same UAM vehicle design in terms of psychoacoustic sound quality metrics (see Section 4).

The design of the UAM vehicle considered in this study is briefly explained in section 2. Section 3 presents the auralization framework employed in this study, including the noise prediction model, the virtual flyover simulation, and the sound synthesis modules. The sound metrics (including conventional and psychoacoustic) considered in this study are explained in section 4, whereas the

listening experiment setup and statistical information about the test subjects are provided in section 5. The main results are discussed in section 6, and the conclusions are drawn in section 7.

2. UAM VEHICLE AND PROPULSION SYSTEM

The UAM aircraft considered in this study is powered by 26 electric, ducted fan engines, where 10 engines are mounted above of the canard wing and 16 above of the main wing. Each engine has a diameter of 0.45 m. Three distinct engine configurations are available: a conventional fan with more stator vanes than rotor blades (baseline), a low-broadband noise fan design (low-broadband), and a low-tonal noise fan design (low-tone) [22]. Both the low-broadband and low-tone designs employ fewer stator vanes than rotor blades. While the aerodynamic performance of all three fans, characterized by similar efficiency, pressure ratio, and thrust, is largely comparable [22], their acoustic characteristics differ, particularly in terms of tonal-to-broadband noise ratio and dominant noise radiation direction [22–24]. These opposing characteristics make them especially suitable for investigating acoustic and psychoacoustic effects as well as their impact on noise perception.

For the present study, the low-broadband fan design is selected due to its tonal-dominated noise radiation. This fan stage consists of 10 stator vanes and 31 rotor blades. As a result of the relatively low number of stator vanes, the broadband noise is reduced by design [22]. Since frequency fluctuations primarily affect tonal noise, the low-broadband fan is well-suited for studying the noise annoyance obtained from rotational speed variations. The fan geometry is depicted in Fig.1(b).

This fan is virtually integrated into the propulsion system of a tilt-duct UAM concept vehicle, which serves as a reference platform for high-fidelity aerodynamic and acoustic studies [23]. The tilt-duct vehicle is visualized in Fig. 1(a). This vehicle can carry a payload of 500 kg over a mission length of 150 km, at a cruise speed of 200 km/h [23]. The design of the vehicle is described in more detail in [23].

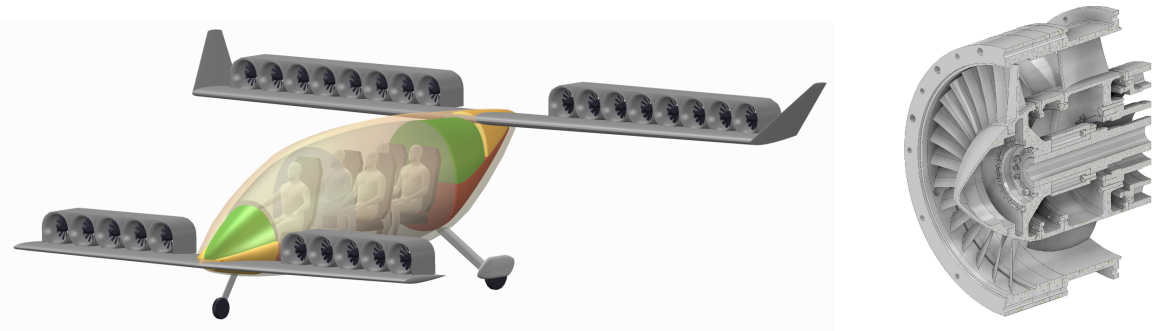

(a) (b)

Figure 1: (a) UAM vehicle concept considered, (b) low-speed, ducted fan engine.

3. AURALIZATION FRAMEWORK

An analytical auralization process is used to obtain the audio files for the listening experiment. This process consists of (1) RANS-informed analytical noise predictions, (2) virtual flyover simulations, and (3) binaural sound syntheses. Detailed descriptions of this process are provided in [24, 25].

3.1. RANS-informed analytical noise prediction

The noise emission is assessed using the in-house tool PropNoise (Propulsion Noise) [8, 26]. PropNoise offers a RANS-informed analytical noise prediction method [8]. A three-dimensional, steady-state RANS simulation is conducted for the low-broadband fan [22]. Based on this numerical simulation, radial distributions of all relevant aerodynamic quantities (e.g. velocity profiles) are extracted. These distributions serve as input for the acoustic module of PropNoise. This module

employs a radial strip approach to compute the acoustic source terms, which are subsequently radially integrated to obtain the in-duct modal sound pressure amplitudes [26]. From these pressure amplitudes, the acoustic modal power is determined. Subsequently, sound propagation through the duct segments and radiation from both the inlet and outlet planes of the fan stage are calculated.

The RANS simulation is carried out at the nominal rotational speed of 4500 rpm and a mass flow rate of 6.98 kg/s. Given that the variations in rotational speed under consideration are small, it is assumed that the streamlines and aerodynamic characteristics remain largely unchanged. Therefore, a single RANS simulation at nominal operating conditions is conducted and used as input for PropNoise.

Before computing the noise emission with PropNoise, rotational speed variations ΔN of $\pm 0.25\,\%$, $\pm 0.5\,\%$, $\pm 1\,\%$, $\pm 2\,\%$, $\pm 3\,\%$, $\pm 4\,\%$ and $\pm 5\,\%$ relative to the nominal speed (4500 rpm) are randomly assigned to the 26 engines. These variations are expected to cause amplitude modulations (or beats) of the blade passing frequency (BPF, accounting for the 31 rotor blades) at modulation frequencies ranging from ± 5.89 Hz to ± 116.25 Hz (for $\Delta N = \pm 0.25\,\%$ to $\pm 5\,\%$, respectively), which may be perceived as a fluctuating sound amplitude sensation [27]. A separate PropNoise calculation is then performed for each engine using its respective rotational speed. The resulting output comprises the directivity patterns for each engine computed on a spherical surface of a defined radius, parameterized by the polar radiation angle. These directivity patterns are assigned to the corresponding engines and serve as input for the virtual flyover simulation.

3.2. Virtual flyover simulation

The in-house tool VIOLIN (Virtual Acoustic Flyover Simulation) enables virtual flyover simulations by propagating noise through the atmosphere to observer positions on the ground [28]. VIOLIN employs a frequency-domain approach to calculate the noise immission. It accounts for the Doppler frequency shift, atmospheric absorption [29], and the influence of atmospheric turbulence on both amplitude and phase relations [30, 31], as well as ground effects including sound wave attenuation and reflection [32].

The trajectory segment for the virtual flyover simulation is selected according to the EASA specifications for VTOL (vertical take-off and landing) aircraft powered by tilting rotors [11]. The "overflight reference procedure" is selected, which is a horizontal flight path with a flight altitude of 150 m. The microphone is placed at a height of 1.2 m centrally under the flight path. The flyover is performed for a simulation time of $t = 22$ s and the trajectory segment is discretized using a time step of $\Delta t = 0.05$ s. The flight Mach number is $M_{\text{flight}} = 0.17$. No changes to the operating conditions occur during the flyover. The speed variations are interpreted as a constant deviation from the nominal rotational speed. Only the noise of the propulsion system is considered for the virtual flyover simulations. The assumption is made that the propulsion system is the dominant noise source, and other noise sources, such as background noise, are neglected. For all 26 fan stages, the initial angular positions of the rotor blades and stator vanes are identical. Regarding the atmospheric conditions, the reference values are specified according to the EASA requirements [11]: the atmospheric pressure is set to 101325 Pa, the ambient air temperature is 25 °C, the relative humidity is 70 % and the wind speed is 0.5 m/s.

The outputs from VIOLIN are frequency- and time-dependent sound pressures at the selected microphone position. Figure 2 depicts two exemplary spectrograms (for the monaural case, i.e. before applying the Head-Related Impulse Responses (HRIRs)) obtained for the cases with $\Delta N = \pm 0\%$ (i.e. all 26 ducted fans operating perfectly synchronized) and $\Delta N = \pm 5\%$ (the case with the most extreme rotational speed fluctuations considered, with a random distribution within $\pm 5\%$ of the nominal rpm value) [21]. The smearing of the tonal energy (highly concentrated for $\Delta N = \pm 0\%$) over a wider frequency band for the case with $\Delta N = \pm 5\%$ is clearly observable. Hence, it is expected that the cases with higher ΔN are perceived as less tonal since, instead of having one very prominent tone, several smaller tones are present. The lack of background noise in the spectrograms (noticeable by

the lack of very low-frequency content) is also apparent.

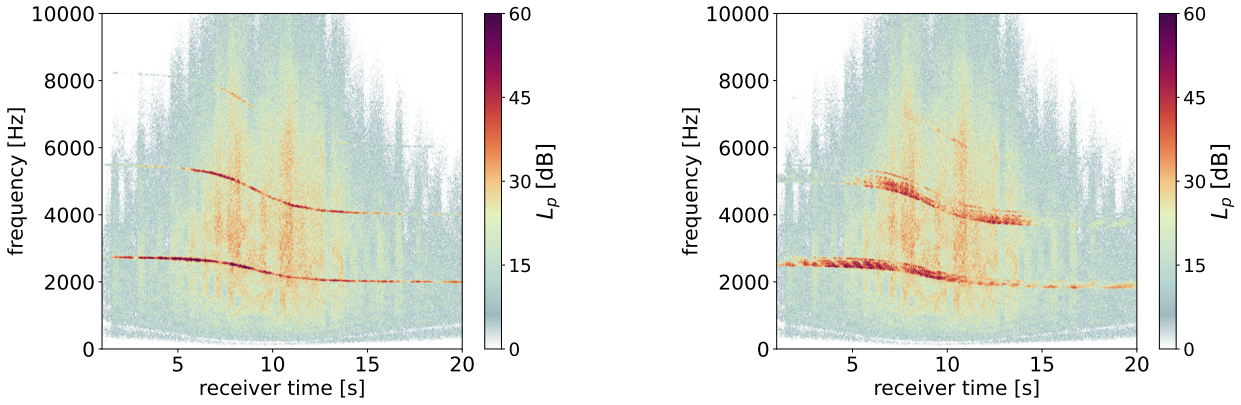

(a) $\Delta N = \pm 0\,\%$. (b) $\Delta N = \pm 5\,\%$.

Figure 2: Spectrograms (monaural sound) at the microphone position of the overflight reference procedure.

3.3. Sound synthesis

The spectrograms determined with VIOLIN are the input for the in-house tool CORAL (Aircraft engine noise auralization) [25]. CORAL provides a binaural noise synthesis to convert the spectrograms into one-dimensional time series for the left and right ears, respectively. The monaural time signals are made stereo by filtering them with HRIRs. For this, a far-field HRIR data set, measured by Bernschütz [33], is considered. As tonal noise sources are assumed to be correlated and broadband sources uncorrelated, CORAL processes these sound components separately. Tonal components are synthesized using an additive approach, while broadband components are generated via a subtractive method, which includes the filtering with a white noise signal, as described in [25]. The resulting audio signals had a duration of 20 s and are saved as Waveform Audio (.wav) files.

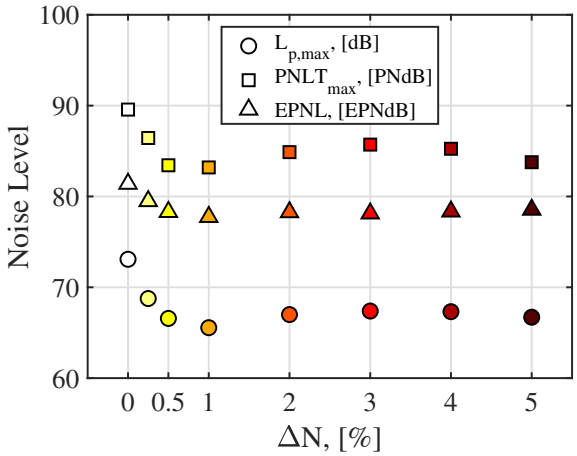

Figure 3: Comparison between maximum L_p, maximum PNLT, and EPNL values at the microphone position of the overflight reference procedure as a function of ΔN. The left ear channel from the binaural sound signals is considered.

Figure 3 contains the maximum L_p, maximum PNLT, and EPNL values at the selected microphone position for all the ΔN cases under consideration. The left ear channel from the binaural sound signals was considered, but the results were almost the same for the right ear as well. As reported in [21], the baseline case with $\Delta N = 0\%$ presents the highest noise levels in all three conventional sound metrics employed. On the other hand, minimum values are achieved around

$\Delta N \approx \pm 1\%$, with values approximately 7.5 dB, 6 PNdB, and 3.5 EPNdB lower than the baseline case.

4. CONVENTIONAL AND SOUND QUALITY METRICS

Conventional sound metrics typically used in noise assessment pose challenges for quantifying noise annoyance [13]. Nevertheless, current noise regulations still employ these metrics for enforcing environmental noise laws. Therefore, the current study considers the A-weighted equivalent sound pressure level $L_{p,A,eq}$, as well as the maximum tone-corrected perceived noise level ($PNLT_{max}$) and the EPNL.

Unlike the sound pressure level L_p metric, which quantifies the purely physical magnitude of sound based on the pressure fluctuations, Sound Quality Metrics (SQMs) describe the subjective perception of sound by human hearing. Hence, SQMs are expected to better capture the auditory behavior of the human ear compared to conventional sound metrics typically employed in noise assessments. The five most commonly-used SQMs [16] are:

- Loudness (N): Perception of sound magnitude corresponding to the overall sound intensity.
- Tonality (K): Perceived strength of unmasked tonal energy within a complex sound.
- Sharpness (S): High-frequency sound content.
- Roughness (R): Hearing sensation caused by modulation frequencies between 15 Hz and 300 Hz.
- Fluctuation strength (FS): Assessment of slow fluctuations in loudness with modulation frequencies up to 20 Hz, with maximum sensitivity for modulation frequencies around 4 Hz.

These five SQMs were calculated for each audio file and combined into global psychoacoustic annoyance (PA) metrics following the model proposed by Zwicker [34], More [35], and Di *et al.* [36]. Henceforth, the top 5% percentiles of these metrics (values exceeded 5% of the time) are reported (and hence the sub-index *5*). The PA metrics are calculated by considering both the top 5% percentiles of the metrics involved (i.e. as a single value per audio), denoted as e.g. $PA_{Zwicker}$, as well as a metric over time, from which the top 5% percentile is calculated, denoted as e.g. $PA_{Zwicker,5}$. All the sound metrics, SQMs, and the PA metrics were computed using the open-source MATLAB toolbox SQAT (Sound Quality Analysis Toolbox) v1.2 [37].

5. LISTENING EXPERIMENT

5.1. Experimental setup

The listening experiment was conducted at PALILA, the Psychoacoustic Listening Laboratory at the Faculty of Aerospace Engineering of Delft University of Technology [38]. The facility consists of a box-in-box soundproof booth with interior dimensions of 2.32 m (length) × 2.32 m (width) × 2.04 m (height). The interior walls, ceiling, and part of the floor are covered with acoustic-absorbing foam panels to prevent sound reflections, see Fig. 4(a). Two bass traps are positioned in diagonally opposing corners to minimise low-frequency noise inside the facility. The facility has free-field sound propagation conditions for frequencies higher than or equal to 1600 Hz and a reverberation time of only 0.07 s. The facility has a weighted average transmission loss of 45 dB and an A-weighted overall background noise level of 13.4 dBA.

The sound reproduction equipment used consists of a *Dell Latitude 7340* laptop equipped with a touchscreen and connected to a pair of *Sennheiser HD560s* open-back headphones. This equipment is calibrated up to 10 kHz, using a *G.R.A.S. 45BB-14 KEMAR* head-and-torso simulator with *G.R.A.S. KB5000 / KB50001 Anthropometric Pinnae*. The reproduction system is accompanied by an open-source, Python-based Graphical User Interface (GUI) [39], allowing this experiment to be self-guided and self-paced.

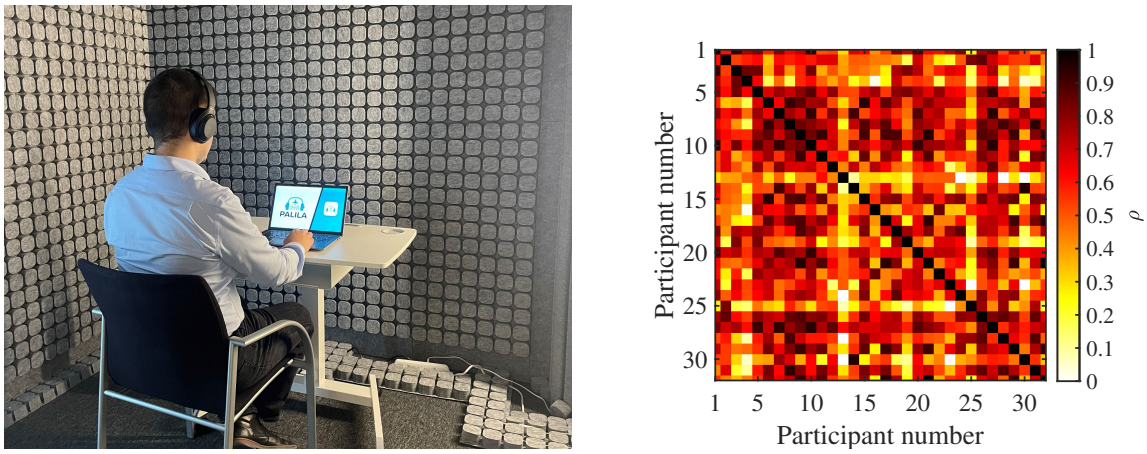

(a) (b)

Figure 4: (a) Example of a listening experiment inside of PALILA. (b) Matrix showing the Pearson correlation coefficients (ρ) between the responses of each pair of individual participants.

After a short briefing about the experiment, participants started the experiment with a questionnaire about their age, gender, employment, and education, as well as questions regarding their hearing health and state of well-being. After answering these questions, participants proceeded to listen to the sound samples and were asked for each sample: "*When you imagine that this is the sound situation in your garden or outdoors, what number from 0 to 10 best shows how much you would be bothered, disturbed, or annoyed by it?*" using an 11-point ICBEN scale. To assess the repeatability of the answers collected, each sound was presented twice. Therefore, each participant listened to a total of 16 stimuli in a randomized order to mitigate, to some extent, potential learning effects. After every four sound samples, participants were given a mandatory 10-s break from listening to alleviate fatigue. After completing the experiment, the participants were provided a 10-euro universal voucher to compensate for their time.

5.2. Test subjects

A total of 32 test subjects participated in the listening experiment, comprising 15 men and 17 women. The average age of the participants was 34.2 years with a standard deviation of 11.1 years.

Regarding the level of education, three participants had a high school diploma as their highest level of education, while the rest held various degrees, such as BSc (2), MSc (21), and PhD (6). The subject group included one student, 29 people employed for wages, one self-employed person, and one retired person. Amongst the *'employed for wages'* group, four individuals worked at Delft University of Technology.

All participants reported feeling well, and their self-reported hearing level was high, with three indicating 'excellent', 13 indicating 'very good', and 15 indicating 'good', and only one indicating 'fair'. None of the participants had ear diseases or wore hearing aids, had a hearing accident in the past, or had ever had tinnitus.

The responses provided by every pair of participants had strong cross-correlations, with average Pearson correlation coefficients of about $\rho = 0.59$, see Fig. 4(b). Moreover, the participant responses were found to be relatively self-consistent, with a root mean square difference of 1.22 points between the responses collected for both repetitions. In general, the absolute differences between the responses for all repeated sounds were below 2 points in 82% of the cases, which is deemed acceptable.

In general, no relevant biases were found between the participants' responses and their demographics; thus, all 32 participants were considered in the psychoacoustic analysis henceforth.

6. RESULTS AND DISCUSSION

The mean annoyance ratings from the listening experiment per rotational speed fluctuation value are presented in Fig. 5(a) for the whole range considered (±0% to ±5%). The responses recorded for the two repetitions per sound are averaged. The standard deviations in the annoyance ratings are depicted as error bars. It is observed that the case with all the 26 fans operating synchronously (i.e. $\Delta N = 0\%$) is perceived as the most annoying, with relatively high average annoyance ratings of approximately 8.5. Increasing ΔN quickly reduces the perceived annoyance, until a plateau is reached around $\Delta N \approx \pm 1\%$ with mean annoyance ratings of approximately 6 out of 10. The case with the largest fluctuations considered (i.e. $\Delta N = \pm 5\%$) seems to present even slightly lower ratings of approximately 5.5. Overall, these results closely follow the same trends observed in several sound metrics previously reported by Schade *et al.* [21].

The percentage of highly annoyed people (%HA, considered as the number of percentage of responses with an annoyance rating of 7 or higher) is depicted in Fig. 5(b). For the reference case ($\Delta N = 0\%$), almost all participants ($\approx 97\%$) are categorized as highly annoyed, but %HA sharply decreases as ΔN increases. Despite an outlier for the case of $\Delta N = \pm 3\%$, the trend is monotonically decreasing and follows relatively well the curve fit depicted as a dashed blue line Fig. 5(b). Whereas the mean annoyance rating for $\Delta N = \pm 3\%$ is relatively similar to other ΔN values nearby, its %HA value is considerably higher. Interestingly, this case presented the lowest tonality of all (see Fig. 6(a)), which may explain why some participants did not find it that annoying. On the other hand, this case presented the highest roughness value (0.11 asper, about four times higher than the $\Delta N = 0\%$ baseline with 0.03 asper). This might be related to the amplitude modulation mentioned in section 1, which, for the $\Delta N = \pm 3\%$ case, it seems to coincide with the most sensitive modulation frequency for roughness (about 70 Hz, according to the Daniel & Webber roughness model [40] considered). On the other hand, roughness as an individual metric has a negative correlation with the annoyance ratings (see Table 1). It is, therefore, difficult to explain the relatively high %HA value for this particular case.

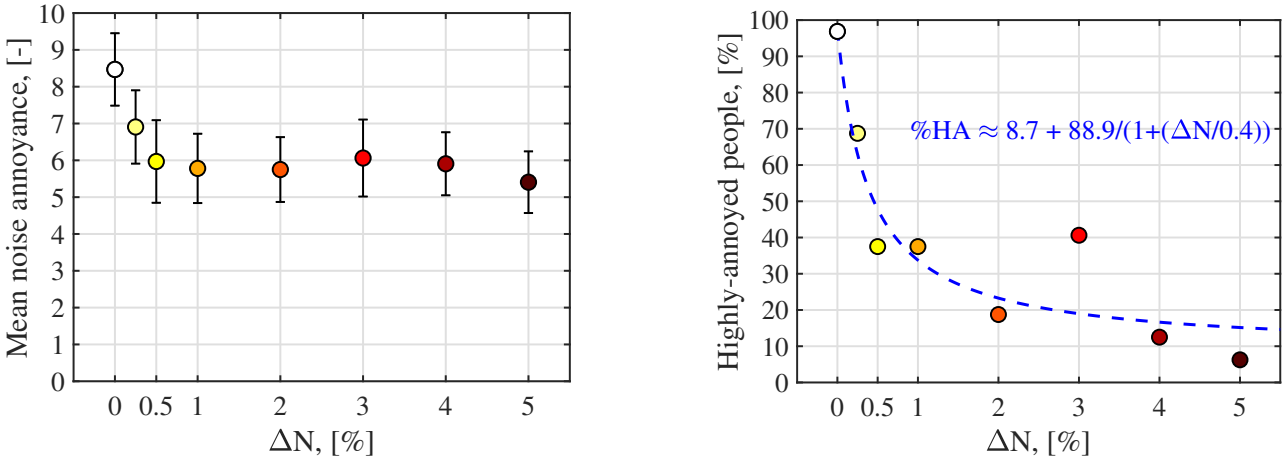

Figure 5: (a) Mean noise annoyance ratings from the listening experiments per audio file with respect to ΔN. The error bars denote the standard deviations in the annoyance ratings. (b) Percentage of highly annoyed people (%HA) with respect to ΔN The dashed blue line represents a curve fit.

The results of the correlation analysis performed between the mean annoyance ratings of the listening experiment and the sound metrics described in section 4 are gathered in Table 1. In particular, the Pearson correlation coefficient ρ (including the 95% confidence interval) and p-value are reported for each metric. All correlations are considered statistically significant (p-value ≤ 0.05), except for S_5, which presented negligible variations (from 2.47 to 2.49 acum, i.e. less than 1%) since the high-frequency content of the sounds considered hardly changed as ΔN varied. Figure 6 depicts the correlation analyses for the best-performing sound quality metric (K_5, Fig. 6(a)), and PA metric

Table 1: Pearson correlation coefficient ρ (including the 95% confidence interval) and associated p-values reported between the mean annoyance ratings and each of the sound metrics and psychoacoustic annoyance models.

Metric	ρ	**p-value**	**Metric**	ρ	**p-value**
$L_{p,A,eq}$	0.938 (0.690 – 0.989)	5.6×10^{-4}	$PNLT_{max}$	0.923 (0.626 – 0.986)	0.001
EPNL	0.947 (0.728 – 0.991)	3.6×10^{-4}	N_5	0.882 (0.469 – 0.979)	0.004
S_5	0.404 (−0.421 – 0.863)	0.321	K_5	0.932 (0.664 – 0.988)	7.3×10^{-4}
R_5	−0.715 (−0.944 – −0.021)	0.046	FS_5	0.830 (0.302 – 0.968)	0.012
$PA_{Zwicker}$	0.913 (0.582 – 0.984)	0.002	$PA_{Zwicker,5}$	0.898 (0.527 – 0.982)	0.002
PA_{More}	0.929 (0.648 – 0.987)	8.6×10^{-4}	$PA_{More,5}$	0.898 (0.526 – 0.929)	0.003
PA_{Di}	**0.952 (0.750 - 0.992)**	2.7×10^{-4}	$PA_{Di,5}$	0.933 (0.666 – 0.989)	7.2×10^{-4}

(PA_{Di}, Fig. 6(b)). In these figures, the corresponding coefficients of determination ρ^2, p-values, and least-squares fits are included.

Despite the relatively coarse frequency resolution (one-third-octave spectra) employed for the assessment of the tonal penalty in the calculation of EPNL, this metric performs reasonably well ($\rho^2 = 0.899$) as an indicator of the mean annoyance ratings. As hypothesized in the discussion of the spectrograms of Fig. 2, tonality (K_5, Fig. 6(a)) considerably decreases when increasing ΔN, reaching values of less than a quarter of the baseline case with $\Delta N = 0\%$ (from ≈ 0.35 to 0.08 t.u.). This metric manages to explain almost 87% of the variation in the annoyance ratings on its own, even outperforming loudness (N_5, $\rho^2 = 0.78$), unlike in recent studies featuring aircraft [41] and drone sounds [13], where loudness was deemed as the best-performing SQM. Nevertheless, the observed reductions in loudness (up to 12.3%) are considerably smaller than those observed for tonality (up to 77%) when increasing ΔN [42]. This fact highlights the relatively high tonal nature of the UAM vehicle sounds considered in this manuscript and the high variance in this aspect within cases. Lastly, the PA model by Di *et al.* (Fig. 6(b)) presents the best overall performance from all the metrics considered, with a minor improvement compared to the EPNL metric ($\rho^2 = 0.906$).

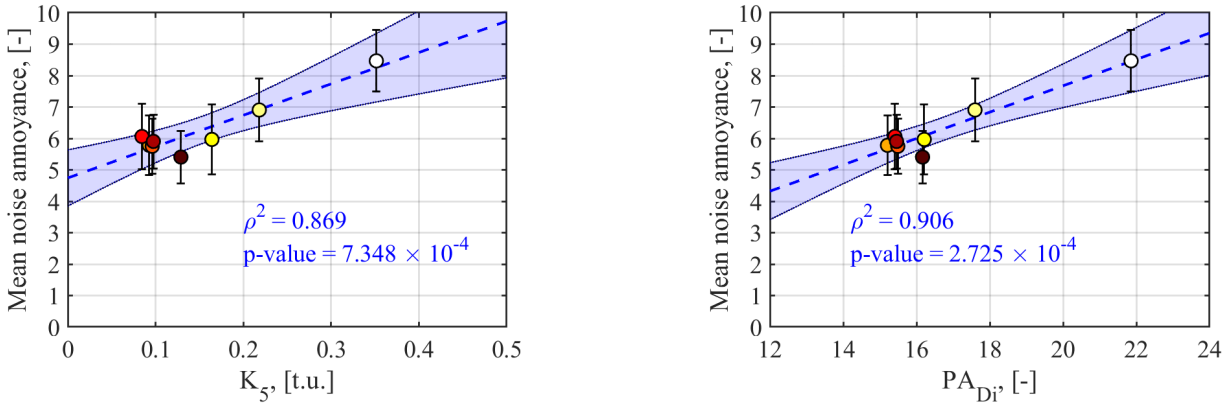

(a) (b)

Figure 6: Correlation analysis between the mean annoyance ratings from the listening experiments and (a) tonality K_5, and (b) the psychoacoustic annoyance (PA) model of Di *et al.*. The error bars denote the standard deviations in the annoyance ratings. The least-squares fits are plotted as dashed blue lines, and the shaded blue areas correspond to the 95% confidence intervals. The corresponding coefficient of determination ρ^2 and p-value are also included.

7. CONCLUSIONS

This manuscript investigated the human perception of a virtual Urban Air Mobility (UAM) vehicle equipped with 26 distributed, ducted, low-speed fans. An auralization framework was employed to obtain the synthetic flyover sounds, including RANS-informed analytical noise predictions, sound propagation through the atmosphere, and the binaural audio rendering at a given observer position.

In particular, this study dealt with the influence of rotational speed fluctuations of the distributed fans ΔN on human perception. This was deemed of interest, since distributed propulsors might be used as a flight control system, and they also may present variations in practice in case not all motors are perfectly synchronized due to practical imperfections.

A listening experiment featuring 32 participants showed that relatively small fluctuations in the rotational speed of the fans (e.g. $\Delta N = \pm 1\%$ with respect to the nominal rotational speed) already reduce the perceived noise annoyance considerably. In general, larger fluctuations in the rotational speed did not seem to continue reducing the mean annoyance rating of the UAM vehicle, at least within the range of variations investigated in this study. Nevertheless, the percentage of highly-annoyed people seemed to follow a relatively monotonically decreasing trend with increasing ΔN. The variations in mean annoyance ratings were relatively well explained by variations in the EPNL and the tonality metrics. Overall, the psychoacoustic annoyance model by Di *et al.* provided the best performance, explaining up to 91% of the variability in the mean annoyance ratings.

Overall, the presence of fluctuations in the rotational speed of distributed propulsors seems to improve (within reasonable limits) the perceived annoyance. Future work should confirm these claims with a more extensive listening experiment campaign, which may also include different fan designs [24].

ACKNOWLEDGEMENTS

The authors would like to kindly thank the participants of the listening experiment for their time and efforts. This publication is part of the project *VIRLWINT* (Virtual acoustical twin of distributed propulsion systems) funded by the German Aerospace Center (DLR). Moreover, this publication is also part of the *Listen to the future* project (project number 20247), a part of the Veni 2022 research programme (Domain Applied and Engineering Sciences). The latter project is granted to Roberto Merino-Martinez and is (partially) financed by the Dutch Research Council (NWO).

REFERENCES

1. F.d.N. Monteiro, R. Merino-Martinez, and L. T. Lima Pereira. Psychoacoustic Evaluation of an Array of Distributed Propellers Under Synchrophasing Operation. In 30^{th} *AIAA/CEAS Aeroacoustics Conference, June 4 – 7 2024, Rome, Italy*, 2024. AIAA paper 2024–3321.
2. Kyle Pascioni and Stephen A. Rizzi. Tonal noise prediction of a distributed propulsion unmanned aerial vehicle. *2018 AIAA/CEAS Aeroacoustics Conference*, 2018.
3. S. Guérin and D. Tormen. A contribution to the investigation of acoustic interferences in aircraft distributed propulsion. *CEAS Aeronautical Journal*, 14:965–982, 2023.
4. M. Boucher, M. Rafaelof, D. Begault, and A. Christian et al. A psychoacoustic test for urban air mobility vehicle sound quality. *SAE Int. J. Adv. Curr. Prac. in Mobility*, 6(2):972–985, 2024.
5. D. Y. Gwak, D. Han, and S. Lee. Sound quality factors influencing annoyance from hovering UAV. *Journal of Sound and Vibration*, 489:115651, December 2020.
6. S. A. Rizzi, D. L. Huff, D. D. Jr. Boyd, P. Bent, Henderson B., K. A. Pascioni, D. C. Sargent, D. L. Josephson, M. Marsan, B. He, and R. Snider. Urban Air Mobility Noise: Current Practice, Gaps, and Recommendations. Technical Report NASA Technical Memorandum 83199, NASA, 2020.
7. Hinnerk Eißfeldt and Maria Stolz. Public perception of air taxis in Germany: anticipated risks,

benefits, and noise sensitivity. *Proceedings of Meetings on Acoustics*, 54(1), 09 2024.

8. R. Jaron. *Aeroakustische Auslegung von Triebwerksfans mittels multidisziplinärer Optimierungen*. Dissertation, German Aerospace Center, Institute of Propulsion Technology, Berlin, Germany, 2018.
9. Davide Giacche, Thomas P. Hynes, Stephane Baralon, John Coupland, Nicholas Humphreys, and Peter Schwaller. Acoustic optimization of ultra-low count bypass outlet guide vanes. *19th AIAA/CEAS Aeroacoustics Conference*, 2013.
10. Annex 16 to the convention on international civil aviation, environmental protection, volume 1, aircraft noise (8th edition). International Civil Aviation Organization. 07 2017.
11. EASA. Environmental protection technical specifications applicable to vtol-capable aircraft powered by tilting rotors. *consultation paper*, 1, 2023.
12. S. A. Rizzi and A. Christian. Psychoacoustic Evaluation of Noise Signatures from Advanced Civil Transport Aircraft. In 22nd *AIAA/CEAS Aeroacoustics Conference, May 30 – June 1 2016, Lyon, France*, 2016. AIAA paper 2016–2907.
13. R. Merino-Martinez, R. M. Yupa-Villanueva, B. von den Hoff, and J. S. Pockelé. Human response to the flyover noise of different drones recorded in field measurements. In 3rd *Quiet Drones conference, September 8 – 11 2024, Manchester, United Kingdom*, 2024.
14. R. Merino-Martinez, I. Besnea, B. von den Hoff, and M. Snellen. Psychoacoustic Analysis of the Noise Emissions from the Airbus A320 Aircraft Family and its Nose Landing Gear System. In 30th *AIAA/CEAS Aeroacoustics Conference, June 4 – 7 2024, Rome, Italy*, 2024. AIAA paper 2024–3398.
15. Yoshiharu Soeta and Hiroko Kagawa. Three dimensional psychological evaluation of aircraft noise and prediction by physical parameters. *Building and Environment*, 167:106445, 2020.
16. G. F. Greco, R. Merino-Martinez, A. Osses, and S. C. Langer. SQAT: a MATLAB-based toolbox for quantitative sound quality analysis. In 52th *International Congress and Exposition on Noise Control Engineering, August 20 – 23 2023, Chiba, Greater Tokyo, Japan*. International Institute of Noise Control Engineering (I-INCE), 2023.
17. R. Merino-Martinez, R. Pieren, B. Schäffer, and D. G. Simons. Psychoacoustic model for predicting wind turbine noise annoyance. In 24th *International Congress on Acoustics (ICA), October 24 – 28 2022, Gyeongju, South Korea*, 2022.
18. R. Merino-Martinez, R. Pieren, and B. Schäffer. Holistic approach to wind turbine noise: From blade trailing–edge modifications to annoyance estimation. *Renewable and Sustainable Energy Reviews*, 148(111285):1–14, May 2021.
19. Randolph Cabell, Robert McSwain, and Ferdinand Grosveld. Measured noise from small unmanned aerial vehicles. *NOISE-CON 2016*, June 2016.
20. M. Vorländer. *Auralization – Fundamentals of Acoustics, Modelling, Simulation, Algorithms and Acoustic Virtual Reality*. Springer, First edition, 2008. ISBN: 978–3540488293.
21. S. Schade, R. Merino-Martinez, P. Ratei, S. Bartels, R. Jaron, and A. Moreau. Initial study on the impact of speed fluctuations on the psychoacoustic characteristics of a distributed propulsion system with ducted fans. *30th AIAA/CEAS Aeroacoustics Conference (2024)*, 2024.
22. S. Schade, R. Jaron, L. Klähn, and A. Moreau. Smart blade count selection to align modal propagation angle with stator stagger angle for low-noise ducted fan designs. *Aerospace*, 11(4), 2024.
23. S. Schade, J. Ludowicy, P. Ratei, M. Hepperle, A. Stürmer, K.-S. Rossignol, S. de Graaf, and T. F. Geyer. Conceptual design of electrically-powered urban air mobility vehicles for aeroacoustic studies. *under review for CEAS Aeronautical Journal, presented at German Aerospace Congress DLRK 2024*, 2025.

24. S. Schade, R. Merino-Martinez, A. Moreau, S. Bartels, and R. Jaron. Psychoacoustic evaluation of different fan designs for an urban air mobility vehicle with distributed propulsion system. *The Journal of the Acoustical Society of America*, 157(3):2150–2167, 03 2025.
25. A. Moreau, A. Prescher, S. Schade, M. Dang, R. Jaron, and S. Guérin. A framework to simulate and to auralize the sound emitted by aircraft engines. *InterNoise conference 2023*, conference proceedings, 2023.
26. A. Moreau. *A unified analytical approach for the acoustic conceptual design of fans for modern aero-engines*. Dissertation, German Aerospace Center, Institute of Propulsion Technology, Berlin, Germany, 2017.
27. A. Osses, R. García León, and A. Kohlrausch. Modelling the sensation of fluctuation strength. In 22^{nd} *International Congress on Acoustics (ICA), September 5 – 9 2016, Buenos Aires, Argentina*, 2016.
28. M. Dang. *Usability and maintainability of the software tools VIOLIN and CORAL*. Bachelor thesis, Baden-Württemberg Cooperative State University, 2022.
29. Attenuation of sound during propagation outdoors, part 1: Calculation of the absorption of sound by the atmosphere. (ISO 9613-1), 06 1993.
30. F. Rietdijk, J. Forssén, and K. Heutschi. Generating sequences of acoustic scintillations. *Acta Acustica united with Acustica*, 103(2):331–338, 2017.
31. A. Prescher, A. Moreau, and S. Schade. Model extension of random atmospheric inhomogeneities during sound propagation for engine noise auralization. *Deutsche Luft- und Raumfahrtkongress - DLRK 2023*, conference proceedings, 2023.
32. Arbeitsgruppe Novellierung der AzB. Anleitung zur Berechnung von Lärmschutzbereichen (AzB). *Umweltbundesamt*, 05 2007.
33. Benjamin Bernschütz. A spherical far field hrir/hrtf compilation of the neumann ku 100. *Proceedings of the 39th DAGA*, pages 592–595, 03 2013.
34. H. Fastl and E. Zwicker. *Psychoacoustics – Facts and models*. Springer Series in Information Sciences, Third edition, 2007. ISBN: 987–3–540–68888–4.
35. Shashikant More and Patricia Davies. Human responses to the tonalness of aircraft noise. *Noise Control Engineering Journal*, 58(4):420–440, 2010.
36. Guo-Qing Di, Xing-Wang Chen, Kai Song, Bing Zhou, and Chun-Ming Pei. Improvement of Zwicker's psychoacoustic annoyance model aiming at tonal noises. *Applied Acoustics*, 105:164–170, 2016.
37. Gil Felix Greco, Roberto Merino-Martínez, and Alejandro Osses. SQAT: a sound quality analysis toolbox for MATLAB, January 2025. v1.2. Zenodo. DOI: 10.5281/ZENODO.14641811.
38. R. Merino-Martinez, B. von den Hoff, and D. G. Simons. Design and acoustic characterization of a psychoacoustic listening facility. In 29^{th} *International Congress on Sound and Vibration (ICSV), July 9 – 13 2023, Prague, Czech Republic*, 2023.
39. J. S. Pockelé. Graphical User Interface for the Psychoacoustic Listening Laboratory (PALILA GUI), March 2025. v1.2.0. Zenodo. DOI: 10.5281/ZENODO.15100497.
40. P. Daniel and R. Webber. Psychoacoustical Roughness: Implementation of an Optimized Model. *Accustica – acta acustica*, 83:113–123, 1997.
41. R. Merino-Martinez and V.S. Buzetelu. Aircraft noise-induced annoyance analysis using psychoacoustic listening experiments. In 11^{th} *Forum Acusticum Euronoise Conference, June 23 – 26 2025, Málaga, Spain*, 2025.
42. A. Osses, G. F. Greco, and R. Merino-Martinez. Considerations for the perceptual evaluation of steady-state and time-varying sounds using psychoacoustic metrics. In 10^{th} *Convention of the European Acoustics Association (Forum Acusticum), September 11 – 15 2023, Torino, Italy*.